Journal of Proteomics 191 (2019) 143–152

Contents lists available at ScienceDirect

Journal of Proteomics

journal homepage: www.elsevier.com/locate/jprot

Global effect of the lack of inorganic polyphosphate in the extremophilic archaeon *Sulfolobus solfataricus*: A proteomic approach

Daniela F. Soto[a], Alejandra Recalde[a], Alvaro Orell[a,b], Sonja-Verena Albers[c], Alberto Paradela[d], Claudio A. Navarro[a], Carlos A. Jerez[a,*]

[a] Laboratory of Molecular Microbiology and Biotechnology, Department of Biology, Faculty of Sciences, University of Chile
[b] Max Planck Institute for Terrestrial Microbiology, Marburg, Germany
[c] Molecular Biology of Archaea, Institute of Biology II-Microbiology, University of Freiburg, Freiburg, Germany
[d] Proteomic Service, CNB-CSIC, Madrid, Spain

ARTICLE INFO

Keywords:
Inorganic polyphosphate
Sulfolobus solfataricus
polyP deficiency
Oxidative stress
ICPL

ABSTRACT

Inorganic polyphosphates (polyP) are present in all living cells and several important functions have been described for them. They are involved in the response to stress conditions, such as nutrient depletion, oxidative stress and toxic metals amongst others. A recombinant strain of *Sulfolobus solfataricus* unable to accumulate polyP was designed by the overexpression of its endogenous *ppx* gene. The overall impact of the lack of polyP on this *S. solfataricus* polyP (−) strain was analyzed by using quantitative proteomics (isotope-coded protein label, ICPL). Stress-related proteins, such as peroxiredoxins and heat shock proteins, proteins involved in metabolism and several others were produced at higher levels in the *ppx* expression strain. The polyP deficient strain showed an increased copper sensitivity and an earlier transcriptional up-regulation of *copA* gene coding for the P-type copper-exporting ATPase. This implies a complementary function of both copper resistance systems. These results strongly suggests that the lack of polyP makes this hyperthermophilic archaeon more sensitive to toxic conditions, such as an exposure to metals or other harmful stimuli, emphasizing the importance of this inorganic phosphate polymers in the adaptations to live in the environmental conditions in which thermoacidophilic archaea thrive.

Significance: Inorganic polyphosphate (polyP) are ubiquitous molecules with many functions in living organisms. Few studies related to these polymers have been made in archaea. The construction of a polyP deficient recombinant strain of *Sulfolobus solfataricus* allowed the study of the global changes in the proteome of this thermoacidophilic archaeon in the absence of polyP compared with the wild type strain. The results obtained using quantitative proteomics suggest an important participation of polyP in the oxidative stress response of the cells and as having a possible metabolic role in the cell, as previously described in bacteria. The polyP deficient strain also showed an increased copper sensitivity and an earlier transcriptional up-regulation of *copA*, implying a complementary role of both copper resistance systems.

1. Introduction

Inorganic polyphosphate (polyP) is a linear polymer of hundreds to thousands of orthophosphate residues linked by high energy phosphoanhydride bonds [1]. PolyP is present in all kinds of organisms: prokaryote and eukaryote and its origin seems to be pre-biotic. In Bacteria and Euryarchaeota, these inorganic polymers are synthetized mainly by the enzyme polyphosphate kinase (PPK) from the terminal phosphate of an ATP molecule in a reversible reaction.

$$(\text{polyP})_n\text{ATP} \overset{\text{PPK}}{\rightleftharpoons} (\text{polyP})_{n+1} + \text{ADP}$$

In Bacteria and Crenarchaeota, the enzyme degrading polyP is the exopolyphosphatase (PPX), that hydrolyses the polymer liberating inorganic phosphate (P_i) [1,2].

$$(\text{polyP})_{n+1} \xrightarrow{\text{PPX}} (\text{polyP})_n + P_i$$

PolyP is involved in a variety of functions in the cell, such as a phosphate reservoir and a substitute for ATP in some kinase reactions. In addition, it is involved in adaptations to different stress conditions, such as virulence, biofilm formation and the detoxification of heavy metals in the cell by chelation [1,2]. It was recently reported that polyP may also act as a primordial inorganic protein chaperone in *Escherichia*

* Corresponding author at: Las Palmeras 3425, Ñuñoa, Santiago 7800003, Chile.
E-mail address: cjerez@uchile.cl (C.A. Jerez).

https://doi.org/10.1016/j.jprot.2018.02.024
Received 1 November 2017; Received in revised form 26 January 2018; Accepted 25 February 2018
Available online 01 March 2018

coli, preventing proteins damage due to reactive oxygen species (ROS) [3].

Sulfolobus solfataricus is a model thermoacidophilic archaeon that lives in a pH range between 2 and 4, and temperatures from 60 to 92 °C and can grow utilizing different carbon sources [4]. One of the advantages of working with this organism is that some tools for its genetic manipulation are available [4,5].

Contrary to other archaea, such as *Sulfolobus metallicus*, *S. solfataricus* does not accumulate polyP in the form of visible granules [6]. The enzyme involved in the synthesis of the polymer is currently unknown in all Crenarchaeotes. However, the PPX enzyme has been described by Cardona et al. [7].

There are few studies related to polyP and its functions in archaea [6,8]. To further study the different roles polyP may have in this domain of life, a global quantitative proteomic analysis of a *Sulfolobus solfataricus* strain deficient in polyP (M16-PPX) was carried out. This mutant strain was generated by the overproduction of its own PPX in the presence of D-arabinose.

2. Materials and methods

2.1. Strains and growth conditions

S. solfataricus strains M16 (*pyr*EF mutant, auxotroph for uracil) [9] and M16-PPX (complemented for *pyr*EF and containing a copy of *S. solfataricus ppx* gene inducible by D-arabinose) were used in this study.

Both strains were grown at 75 °C with shaking at 120 rpm in Brock Medium (1.3 g/L $(NH_4)_2SO_4$, 0.28 g/L KH_2PO_4, 0.25 g/L $MgCl_2 \times 7\ H_2O$, 0.07 g/L $CaCl_2 \times 2\ H_2O$, 0.02 g/L $FeCl_2 \times 4\ H_2O$, 1.8 mg/L $MnCl_2 \times 4\ H_2O$, 4.5 mg/L $Na_2B_4O_7 \times 10\ H_2O$, 0.22 mg/L $ZnSO_4 \times 7\ H_2O$, 0.06 mg/L $CuCl_2 \times 2\ H_2O$, 0.03 mg/L $Na_2MoO_4 \times 2\ H_2O$, 0.03 mg/L $VoSO_4 \times 2\ H_2O$ and 0.01 mg/L $CoCl_2 \times 6\ H_2O$), pH 3 and supplemented with 0.1% (p/v) N-Z amine (Fukla®), 0.2% (p/v) glucose and with 0.01 mg/mL uracil only in the case of M16 strain.

The recombinant PPX production was induced by adding 0.2% (w/v) D-arabinose (Sigma-Aldrich®).

2.2. Construction of recombinant Sulfolobus solfataricus M16-PPX

2.2.1. Subcloning of ppx gene from S. solfataricus (ppxS.so) in pMZ1

The procedures to generate the recombinant *S. solfataricus* M16-PPX were essentially as described before [5]. The *ppx* gene was amplified from *S. solfataricus* P2 genomic DNA by using PCR and the primers 5′ppxS.so*Nco*I: 5′CCATGGTATCGGCAGTTATAGATTG and 3′ppxS.so-*Bam*HI: 5′GGATCCTACTCTTACACCGACAACG. The product obtained was ligated to Pcr2.1-TOPO (Invitrogen®) by using 25 ng of the vector and 10 ng of the purified PCR product obtained by electrophoretic separation in an agarose gel. Ligation was carried out at room temperature for 30 min in a final volume of 6 μL. Two microliter of this reaction mix were used to transform chemocompetent *E. coli* JM109 following manufacturer's instructions. Plasmid Pcr2.1-TOPO-ppxS.so was purified from a positively transformed clone selected by PCR. 0.5 μg of this plasmid was digested with *Nco*I and *Bam*HI, using Tango 1× Buffer (Fermentas) in a final volume of 20 μL by incubating during 2 h at 37 °C. The digestion product (50 ng) was ligated to 25 ng of pMZ1 vector, previously digested with the same restriction enzymes, by using T4 DNA ligase 1× buffer and 5 U of T4 DNA ligase. After incubating for 2 h at 37 °C, 5 μL of this ligation reaction product were used to transform chemocompetent *E. coli* JM109. Transformed colonies were selected with ampicillin and verified by PCR. Plasmid pMZ1-*ppxS.so* was purified and the identity of the *ppx* gene was determined by sequencing both DNA strands.

2.2.2. Cloning of recombinant ppxS.so gene (r_ppxS.so) into the expression vector pMJ0503

The binary vector pMJ0503 (for *E. coli* and *S. solfataricus*) [5,10] was used to over-produce PPX in *S. solfataricus*. This vector integrates into the *S. solfataricus* genome and contains the *pyrEF* gene as a selection marker. First, pMZ1-ppxS.so was digested with 4 U of *Bln*I and *Eag*I, in NEB3 buffer 1× (New England Biolabs) for 3 h at 37 °C and the product obtained was purified after its separation by agarose gel electrophoresis. Vector pMJ0503 was digested with the same restriction enzymes under identical conditions. Forty ng of the digestion product and 5 ng of digested pMJ0503 vector were mixed with T4 DNA ligase buffer 1× and 5 U of T4 DNA ligase. Ligation reaction was carried out for 16 h at 4 °C. Five μL of the ligation mix was used to transform *E. coli* Stable4 (Stratagene®), according to the manufacturer's instructions. Positive clones were selected with ampicillin by employing colony PCR and the primers designed for *ppxS.so*. Finally, pJ0503-r_ppxS.so was sequenced for DNA identity verification.

2.2.3. Transformation of S. solfataricus M16 with pJ0503-r_ppxS.so

Transformation of cells was done by electroporation. Fifty milliliter of *S. solfataricus* M16 (uracil auxotroph) grown until exponential phase (0.3 OD_{600} nm) were centrifuged for 30 min at 4 °C at 2800 ×*g*. Cells obtained were washed several times with 20 mM saccharose, pH 5.6 to eliminate salts. Finally, cells were resuspended in the same saccharose solution at 10^{10} cells/mL.

Fifty microliter aliquots of the cells suspension were mixed with 150, 300 or 450 ng of plasmid pJ0503-*r_ppxS.so* and transferred to BioRad electroporation cuvettes, where electroporation was carried out under the following conditions: 1,5 kV, 25 μF and 400 Ω. Next, the cells suspension was diluted into 1 mL of fresh Brock medium supplemented with 0.1% N-Z amine and were further incubated for 1 h at 75 °C with vigorous agitation. Cells were then transferred to 50 mL of Brock medium supplemented with 0.1% N-*Z*-amine and 0.01 mg/mL uracil and grown for 2–3 days until 0.5 OD_{600} nm was reached. To select non-auxotrophic cells for uracil, aliquots from the previous culture where used to inoculate fresh Brock medium with only N-Z amine as supplement. Cells grown in this medium were induced in the presence of D-arabinose to verify the overproduction of PPX. Finally, aliquots of the cells suspension were stored in 20% glycerol at −80 °C.

2.3. Production and purification of recombinant PPX (rPPX)

To induce the production of rPPX, *S. solfataricus* M16-PPX cells were grown up to 0.4 OD_{600} nm, followed by the addition of 0.2% D-arabinose and further incubation for 4 h. Cells were then collected by centrifugation and resuspended in sonication buffer (50 mM Tris–HCl pH 8.5, 10 mM EDTA) containing phenylmethylsulfonyl fluoride (PMSF) as protease inhibitor (100 μg/mL). Cells were then disrupted by sonication on ice (Ultrasonic Liquid Processor, SONICATOR®), using 9 cycles of 20 s pulses with 30 s of pauses in between. The lysate was centrifuged at 100,000 ×*g* for 1 h at 4 °C and 5 mL of the supernatant was applied to a column containing 1 mL of his-NTA resin with $NiSO_4$ (Sigma-Aldrich). The column was washed three times with 800 μL of wash buffer (50 mM Hepes pH 8.5, 50 mM KCl and 30 mM Imidazole). Finally, rPPX was eluted in 3 fractions of 400 μL elution buffer (50 mM HEPES pH 7.0, 50 mM KCl and 250 mM Imidazole). Fractions of 0.5 mL were collected and analyzed by SDS-PAGE and Western blot by using rabbit monoclonal antibodies against His tag.

2.4. PolyP extraction from S. solfataricus cells

Cells from a 5 mL culture were collected by centrifugation for 5 min at 4500 ×*g*. The pellet was resuspended in 0.3 mL of 4 M guanidine isothiocyanate (GITC), 50 mM Tris-HCl pH 7.0 prewarmed at 95 °C as previously described [1,6]. The suspension was agitated in vortex and heated at 95 °C for 3 min. Twenty μL of each sample was saved for protein quantification with Coomassie Plus Protein Assay Reagent (PIERCE). 30 μL of 10% SDS was added to each sample and then they were heated again at 95 °C for 5 more min. 300 μL of ethanol (100%)

and 5 μL of silica (Glassmilk) was added and mixed by vortexing followed by heating at 95 °C for 30 s. After 1 min centrifugation at 13,000 x g, the supernatant was removed and the glassmilk pellet containing polyP, DNA and RNA was resuspended in 200 μL of cool New Wash Buffer (5 mM Tris-HCl pH 7.5, 50 mM NaCl, 5 mM EDTA, 50% ethanol). After centrifugation, glassmilk was finally resuspended in 100 μL of a solution containing 50 mM Tris-HCl pH 7.0, 5 mM $MgCl_2$, 5 μg/mL DNase and 5 μg/mL RNase and incubated for 30 min at 37 °C. The pellet was washed twice with New Wash Buffer and polyP was recovered from the glassmilk after repeatedly vortexing it with 50 μL of water, heating at 95 °C and centrifugation. Finally, a total of 100 μL of polyP-containing solution was obtained and frozen at −20 °C for later quantification.

2.5. Enzymatic determination of polyP content

Thirty microliter of polyP containing solution was used for quantification. The polymers were subjected to acid hydrolysis with 2 N HCl (30 μL) for 30 min at 95 °C to release inorganic phosphate (P_i). Quantification of total P_i was done with EnzChek Phosphate Assay kit (Invitrogen) following manufacturer's instructions and expressed as nmol of P_i per mg of protein.

2.6. Total protein extracts preparation for proteomic analysis

After 24 h of growth in the absence of polyP, cells were harvested by centrifugation (7700 × *g* for 15 min). The cell pellets were washed three times with Brock's medium and lysed by sonication as described in Section 2.3. The lysate was centrifuged at 9800 × *g* for 5 min to eliminate unbroken cells and cell debris. Total protein concentration in the cell-free extract was determined by using the Coomassie Plus Protein Assay Reagent (PIERCE).

Fifty micrograms from each of three biological replicates were mixed to obtain a triplicate representative sample with a total of 150 μg of protein from each experimental condition. These samples were lyophilized for 48 h at −40 °C and stored at −20 °C until they were labeled with isotope-coded protein label (ICPL).

2.7. Protein digestion and ICPL-labeling

The ICPL reagent protocol was optimized for labeling 100 μg of each individual sample per experiment. Thus, 100 μg of total protein extracts was individually dissolved in 8 M urea, 25 mM ammonium bicarbonate, reduced with 10 mM dithiothreitol and alkylated with 50 mM iodoacetamide. The urea concentration was reduced to 2 M with 25 mM ammonium bicarbonate and the sample was digested overnight at 37 °C with trypsin (Roche Diagnostics GmbH, Mannheim, Germany) in a sample:protease ratio of 25:1. Before ICPL-labeling, salts and urea were removed by using high-capacity OMIX C18 tips (Varian, Palo Alto, CA). Sample labeling with the light and heavy versions of the ICPL reagent (Serva Electrophoresis, Heidelberg, Germany) was performed at the peptide level according to the manufacturer's instructions.

2.8. 2D-nano LC ESI-MS/MS analysis

After ICPL-labeling samples were combined (200 μg per experiment) and dissolved in 100 μL of 10 mM NH_4OH in water, pH 9.5 and fractionated in a wide-pH range 5 μm particle size, 100 × 2.1 mm reversed phase XBridge column (Waters, Wexford, Ireland) using a Knauer Smartline HPLC system. Conditions for gradient elution, flow rate, injection volumes, number of HPCL fractions and second dimension of the 2D-nano LC ESI-MS/MS analysis were carried out as previously reported [11].

2.9. Protein identification and quantitative analyses

MS and MS/MS data obtained for individual HPLC fractions were merged using the Analysis Combiner tool and subsequently processed as a single experiment using DataAnalysis 3.4 (Bruker Daltonics, Bremen, Germany). In most cases, an accuracy of ± 0.1–0.2 Da was found both for MS and MS/MS spectra. For protein identification, MS/MS spectra (in the form of Mascot generic files) were searched against the *S. solfataricus* P2 UniprotKB forward-reversed database. (http://www.uniprot.org). Sequence reversal was done using the program DBToolkit v4.1.5. Database searches were done using a licensed version of Mascot v.2.2.04 (www.matrixscience.com; Matrix Science, London, UK). Search parameters were as previously described [12]. FDR ≤ 5% for peptide identification were manually assessed as follows: after database searching, peptide matches were ranked according to their Mascot scores. This list contains peptide sequences matching either forward or reversed database sequences. Then, a subset containing 5% of peptides matching the reversed sequences was extracted.

Qualitative and quantitative analyses were performed by using the software WARP-LC 1.1 (Bruker Daltonics, Bremen, Germany). After peptide identification, the software calculates the extracted ion chromatogram for the putative ICPL-labeled pair according to: (a) the mass shift defined by the labeling reagent, (b) a mass tolerance of 0.5 Da, and (c) a retention time tolerance of 40 s. Relative ratios between light and heavy ICPL-labeled peptides were calculated based on the intensity signals of their corresponding monoisotopic peaks, and according to these individual peptide ratios the software calculates the protein ratio.

2.10. Total RNA extraction from S. solfataricus and cDNA synthesis

To study the expression of genes of interest, cells were grown until they reached exponential growth phase (0.3 OD_{600} nm) and were supplemented with 0.2% D-arabinose. After 3 h of induction, 1 mM $CuSO_4$ was added and cells were collected (10 mg wet weight) at different times and lysed as previously described [13]. RNA was extracted by using TRIzol (Invitrogen®) as described by the manufacturer. Remaining DNA was eliminated by adding 40 U of TURBO DNA-free DNase (Ambion®) following manufacturer's instructions. 0.8 μg of total RNA was reverse transcribed for cDNA synthesis. The reaction was performed by using ImProm-II (Promega) reverse transcriptase, 0.5 μg of random hexamers (Promega) and 3 mM $MgCl_2$ for 1 h at 42 °C. Three biological replicas were used for every experimental condition.

2.11. Primer design and real-time RT-PCR

Primers for qRT-PCR were designed by using the annotated genome of *S. solfataricus P2* and Primer3 Software, and were synthetized by Invitrogen. To check primer specific annealing and optimal melting temperature, PCR reactions were carried out with Taq DNA polymerase from Promega following manufacturer's instructions and the products were separated by gel electrophoresis (1% w/v agarose). Gene expression was analyzed with Corbett Rotor Gene 6000 system (Corbertt Research®), using 7.5 μL QuantiFast SYBR Green (Qiagen®) master mix, 1 μL of primer and 1 μL of a 1:20 dilution of the cDNA. *rps2P* was selected as housekeeping gene and Cq values of each transcript of interest were standardized to the Cq value of *rps2P*. At least 2 technical replicates per qRT-PCR reaction were performed.

The efficiency of each primer pair was calculated from the average slope of a linear regression curve, which resulted from qPCRs using a 10-fold dilution series (10 pg–10 ng) of *S. solfataricus* chromosomal DNA as template. Efficiencies between 90 and 110% were used. Cq values (quantification cycle) were automatically determined by Real-Time Rotor-gene 6000 PCR software (Corbett Life Sciences/Quiagen company) after 40 cycles. Cq values of each transcript of interest were standardized to the Cq value of the *rps2P* gene. At least 3 biological replicates of each assessed condition and 2 technical replicates per

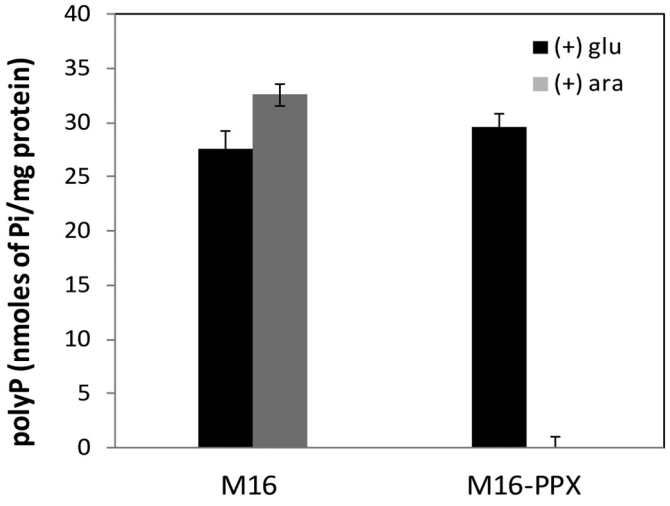

Fig. 1. PolyP levels in *S. solfataricus* recombinant strain M16-PPX. *S. solfataricus* strains M16 and M16-PPX were grown in the presence of 0.2% D-arabinose (+ara) or 0.1% glucose (+glu). Cells were harvested at the early stationary phase and polyP was extracted and quantified. Three independent determinations were performed. The error bars represent the standard deviations.

qPCR reaction were performed.

2.12. Statistical analysis

Data obtained was subjected to analysis of variance (ANOVA) and a Bonferroni's test.

3. Results and discussion

3.1. M16-PPX strain overproduces PPX enzyme and lacks polyP

Strains M16 and M16-PPX were grown in the presence of either 0.1% glucose or 0.2% D-arabinose until the early stationary phase was reached. As shown in Fig. 1, polyP levels in M16 and M16-PPX were very similar when both strains were grown in the presence of glucose. However, in the presence of D-arabinose polyP levels were not detectable in M16-PPX. On the other hand, polyP levels in M16 remained the same when grown either in glucose or D-arabinose.

To determine the time it takes PPX to deplete polyP from the cells, *S. solfataricus* M16-PPX was grown until early exponential phase (0.3 OD_{600} nm) and was induced in the presence of D-arabinose. PolyP levels were measured at different times after induction. After 2.5–3 h, the polyP content in M16-PPX strain was not detectable by the method described in Section 2.5 (data not shown).

3.2. Quantitative proteomics

For proteomics analysis, proteins were extracted from *S. solfataricus* M16-PPX and the control M16 strain, both induced in the presence of D-arabinose for 24 h.

Fifty three proteins changed their levels in the polyP (−) construction. Twenty-nine proteins were up-regulated and 24 down-regulated. Metabolism was the functional category that included most of the changes in protein abundance in cells lacking polyP (Fig. 2). Thirty-four of them (64.2%) changed their levels in this functional category. "Energy production and conversion" was the subcategory with the greatest number of variations. This agrees with polyP being a source of phosphate for many enzymes, as previously described in bacteria [1].

"Information storage and processing" corresponded to the general category with the second number of changes (13 proteins or 24.5% of total). Meanwhile, 4 (7.5%) proteins of unknown function changed their levels in the absence of polyP.

3.2.1. Changes in carbohydrates and lipids transport and metabolism, and energy production and conversion related proteins

Amongst the up-regulated proteins (Table 1) there was an alpha amylase (SSO0988). This enzyme degrades glycogen and releases glucose to the intracellular medium to be incorporated into the energetic pathways (see Fig. 3). It was also reported that glycogen is a polysaccharide reservoir in thermoacidophilic archaea [14].

In the "Energy production and conversion" category, two subunits of the carbon monoxide dehydrogenase enzyme (small chain SSO2433 and large chain SSO2091) were overproduced (Table 1). This enzyme catalyzes the conversion of CO to CO_2, and can also act as an acetyl-CoA synthase [15] generating acetyl-CoA which can be integrated into the TCA cycle (Fig. 3, in "other reactions of interest").

Regarding the respiratory chain, a rise in the levels of an NADH dehydrogenase D subunit (SSO0324) was determined (Table 1) (bottom part of Fig. 3). The respiratory NADH dehydrogenase is an essential component of many bacterial respiratory chains. In *S. solfataricus* there is an activity apparently derived from a cytoplasmic flavin-containing NADH oxidase [16]. It also contains genes encoding for an NADH dehydrogenase core (SSO0665, SSO0322-0329) forming a *nuoBCDHIL* operon that would be partially equivalent to the one present in *E. coli*. It was described that the transcription of *nuoBCDHIL* operon increased after thermic stress in *S. solfataricus* [17]. Depletion of NADH levels is a

Funtional Category	n° prot.	prot. (+)	prot. (-)	%
Metabolism	**34**	**18**	**16**	**64.2**
Energy production and conversion	8	4	4	15.1
Amino acid transport and metabolism	7	4	3	13.2
Nucleotide transport and metabolism	3	3	0	5.7
Carbohydrate transport and metabolism	7	2	5	13.2
Coenzyme transport and metabolism	4	3	1	7.5
Lipid transport and metabolism	4	2	2	7.5
Secondary metabolites biosynthesis, transport and catabolism	1	0	1	1.9
Cellular processes and signaling	**2**	**0**	**2**	**3.8**
Cell wall/ Membrane/ Envelope biogenesis	1	0	1	1.9
Defense mechanism	1	0	1	1.9
Information storage and processing	**13**	**11**	**2**	**24.5**
Translation ribosomal structure and biogenesis	2	2	0	3.8
Transcription	7	5	2	13.2
Replication, Recombination and Repair	1	1	0	1.9
Postranscriptional modification, Protein Turnover, Chaperones	3	3	0	5.7
Poorly Characterized	**4**	**0**	**4**	**7.5**
General function predicted only	4	0	4	7.5
TOTAL	**53**	**29**	**24**	**100.0**

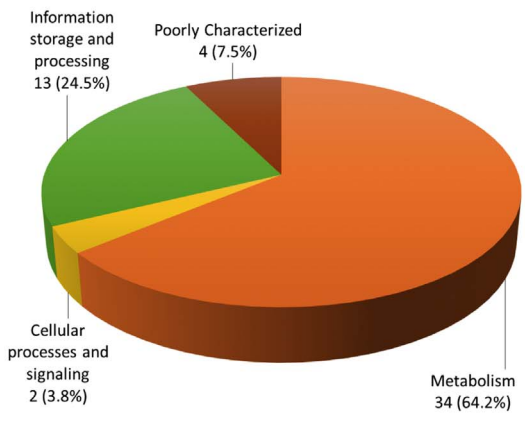

Fig. 2. Functional categories and number of *S. solfataricus* proteins changing their levels in M16-PPX (polyP−) compared to M16 (polyP+) as detected by ICPL total proteomics. (+) Indicates up-regulated and (−) down-regulated proteins. Pie chart refers to proteins listed in the table.

Table 1
More abundant proteins in *Sulfolobus solfataricus* M16-PPX, lacking polyP, compared *to S. solfataricus* M16.

Accession number	ORF	Function/similarity	Score[a]	Coverage (%)	Peptide number	Fold change (PolyP − /PolyP +)
Metabolism						
Carbohydrate transport and metabolism						
Q97ZD2	SSO0988	Alpha amylase	96.43	5.37	1	2.22
Q97U20	SSO3205	Uncharacterized protein	45.98	15.52	1	1.9
Energy production and conversion						
Q97W14	SSO2433	Carbon monoxide dehydrogenase, small chain ((CutC-1)	130.68	30.41	5	2.53
Q7LXA2	SSO2091	Carbon monoxide dehydrogenase, large chain (CutA-2)	64.08	7.88	2	2.23
Q980H3	SSO0324	NADH dehydrogenase subunit D (NuoD)	61.92	11.95	3	2.17
Q97V19	SSO2817	Electron transfer flavoprotein, alpha and beta-subunit (EtfAB/fixAB)	130.08	18.03	8	1.75
Lipid transport and metabolism						
Q97YZ3	SSO1156	Acyl-CoA dehydrogenase related protein (Acd-like1)	44.48	23.68	2	5.95
Q97VU9	SSO2508	Acetyl-CoA *c*-acetyltransferase (Acetoacetyl-CoA thiolase) (AcaB-6)	100.21	10.79	4	1.92
Nucleotide transport and metabolism						
Q7LWG1	SSO1193	Exopolyphosphatase			4	1.27
Q980P6	SSO0241	5-formaminoimidazole-4-carboxamide-1-(beta)-D-ribofuranosyl 5′-monophosphate synthetase	72.2	31.23	7	1.96
Q9UX24	SSO0629	Phosphoribosylformylglycinamidine synthase, subunit PurL	108.93	17.21	4	1.95
Coenzyme transport and metabolism						
Q97WC7	SSO2303	Probable cobalt-precorrin-6B C(15)-methyltransferase	45.1	17.09	1	3.58
P95999	SSO0061	Geranylgeranyl diphosphate synthase	64.74	13.55	2	3.58
Q97ZK1	SSO0905	D-3-phosphoglycerate dehydrogenase (SerA-1)	82.11	23.01	5	1.96
Amino acid transport and metabolism						
Q97VM5	SSO2597	Serine-pyruvate aminotransferase (AgxT)	84.88	14.58	3	2.88
Q97WV4	SSO2008	*N*-methyl hydantoinase A (HuyA-2)	88.68	6.21	2	2.44
Q97UR6	SSO2936	*N*-methylhydantoinase A (HyuA-3)	88.68	8.77	2	2.44
Q97U16	SSO3210	Acetolactate synthase large subunit homolog (IlvB6)	116.57	6.81	4	1.64
Secondary metabolites biosynthesis, transport and catabolism						
Q97UR3	SSO2939	Maleate cis-trans isomerase, probable (MaiA)	48.04	9.09	2	0.58
Information storage and processing						
Translation, ribosomal structure and biogenesis						
Q980V0	SSO5343	RNA-binding protein	49.49	40	2	2.03
Q980Q5	SSO5479	30S ribosomal protein S28e	79.23	22.89	1	1.79
Transcription						
Q97ZF4	SSO6877	DNA/RNA-binding protein Alba 2	138.69	52.81	5	4.89
P58111	SSO0446	Transcription initiation factor IIB 1	87.73	10.36	2	3.12
P60849	SSO0962	DNA/RNA-binding protein Alba 1	1176.8	30.93	5	2.36
Q980R4	SSO0220	Transcription termination protein NusA	99.25	25	2	2.24
Q980S8	SSO5410	Small nuclear riboprotein protein (SnRNP-1)	106.65	39.08	5	1.71
Replication, recombination and repair						
Q97ZE3	SSO6901	Chromatin protein Cren7	204.72	76.67	24	3.3
Postranscriptional modification, protein turnover, chaperones						
Q97VL0	SSO2613	Peroxiredoxin (Bcp-4)	362.81	33.97	46	3.2
Q97VJ4	SSO10788	TusA-related sulfurtransferase	47.24	32.47	3	2.43
P95895	SSO2121	Peroxiredoxin (Bcp-2)	190.77	50.23	12	1.75

[a] Score in this table refers to protein score, according to Mascot search engine.

desirable situation to alleviate oxidative stress in microorganisms [18], since its passage through the respiratory chain generates ROS. Electron transfer flavoprotein (SSO2817) was also found up-regulated (not shown in Fig. 3).

In the “lipid transport and metabolism” category (Table 1), the acyl-CoA dehydrogenase related protein (Acd-like 1) increased its levels (SSO1156, not included in Fig. 3). This change can be related in several microorganisms to an increased rate of fatty acid degradation and a subsequent production of acetyl-CoA. This metabolite might be channeled to the TCA cycle to produce ATP via substrate-level phosphorylation, alleviating oxidative stress if oxidative phosphorylation, is used instead [18].

Concerning down-regulated proteins in Table 2, five proteins are listed in the “Carbohydrate transport and metabolism” category. Alpha-glucosidase (SSO3051) decreased its levels (Fig. 3, upper part). This enzyme was demonstrated to prefer glycogen as substrate, instead of maltose or other polysaccharides [19]. It is possible that under the experimental condition, this protein would be unnecessary, and the microorganism might prefer the alpha amylase (SSO0988) (Fig. 3, upper part), because it is more specific for glycogen degradation. Table 2 also shows a reduction in the levels of a maltose ABC transporter, maltose binding protein (SSO3053, category Amino acid transport and metabolism) and in an arabinose ABC transporter, arabinose binding protein (SSO3066, category Carbohydrate transport and metabolism: see upper part of Fig. 3). This situation was previously reported in the heat shock response of *S. solfataricus* by Tacholjian and Kelly [17]. Because these transporters consume ATP to internalize sugars, a down regulation of these proteins could imply enough glucose generation by glycogen hydrolysis.

The levels of phosphoenolpyruvate synthase (SSO0883) (Fig. 3) an enzyme involved in gluconeogenesis decreased in the absence of polyP (Table 2). Probably this was to avoid spending energy in the synthesis of new glucose molecules.

Concerning the Pentose Phosphate Pathway, only a decrease in Ribose 5-phosphate isomerase (RpiA) (SSO0978) was observed (Table 2 and upper right portion of Fig. 3). Finally, in the carbohydrate metabolism category, an uncharacterized protein (SSO3029) with a xylose-isomerase domain predicted was down-regulated in the absence of polyP (not included in Fig. 3).

Although no enzymes directly involved in the TCA cycle changed under the condition studied, there were some enzymes whose reaction products are related to this cycle. The decrease in the levels of malate

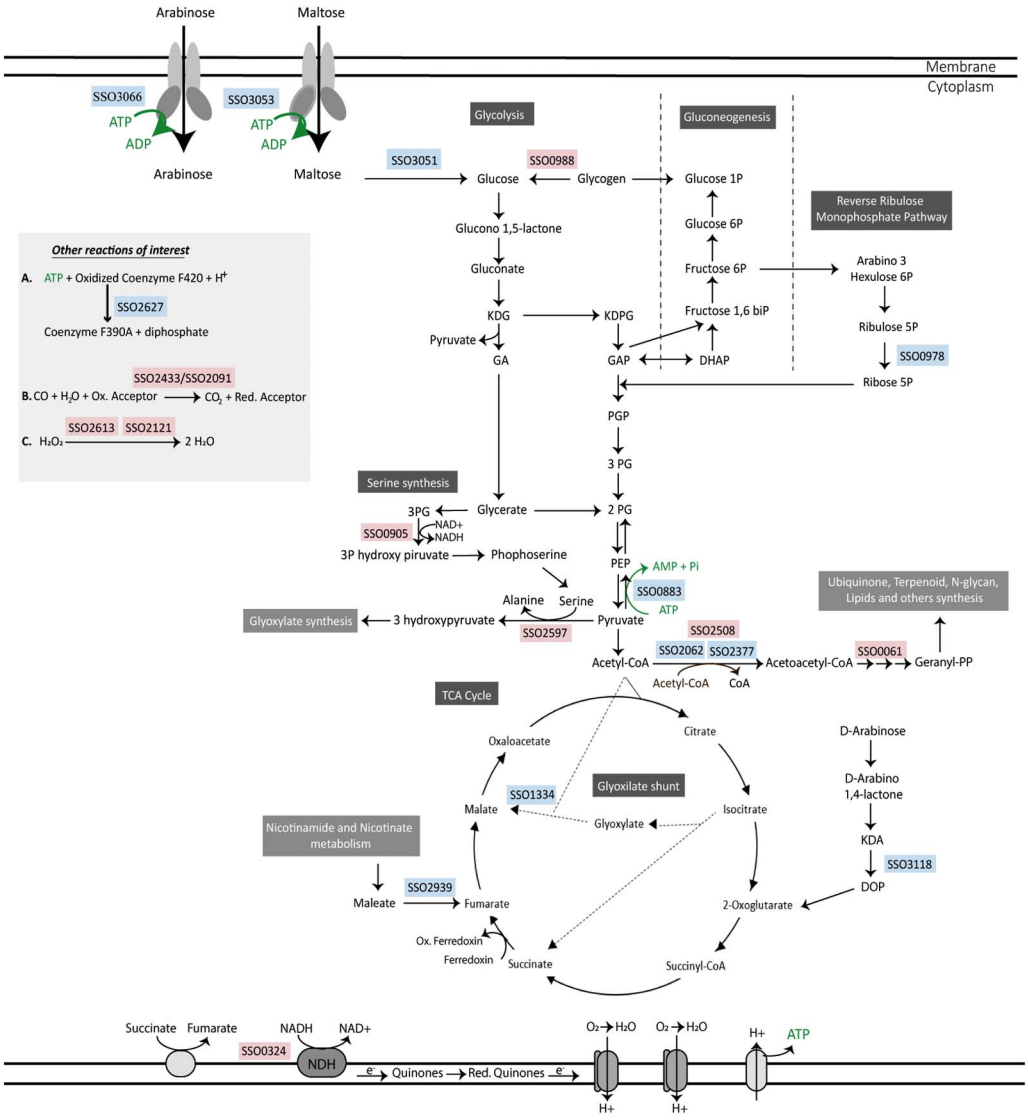

Fig. 3. Proteins changing their levels in some metabolic pathways due to the absence of polyP in *S. solfataricus* cells. Enzymes up regulated are indicated by pink rectangles: Alpha amylase (SSO0988), Serine-pyruvate aminotransferase (SSO2597), Acetyl-CoA *c*-acetyltransferase AcaB-6 (SSO2508), SerA-1 (SSO0905), Geranylgeranyl pyrophosphate synthase (SSO0061), NADH dehydrogenase D subunit (SSO0324), Peroxiredoxins Bcp-2 (SSO2121) and Bcp-4 (SSO261), Carbon monoxide dehydrogenase, small chain (SSO2433) and large chain (SSO2091). Down-regulated proteins are indicated by light blue rectangles: Alpha-glucosidase (SSO3051), Arabinose transporter (SSO3066) Maltose transporter (SSO3053), Phosphoenolpyruvate synthase (SSO0883), Malate synthase (SSO1334), Maleate isomerase (SSO2939), Ribose 5-phosphate isomerase (SSO978), Acetyl-CoA *c*-acetyltransferase AcaB-3 (SSO2062), AcaB-4 (SSO2377), 2-dehydro-3-deoxy-D-arabinonate dehydratase (SSO3118), CoA-ligase/coenzyme F390 synthetase (SSO2627). (For interpretation of the references to color in this figure legend, the reader is referred to the web version of this article.)

synthase (SSO1334) (Table 2, Fig. 3) may increase the TCA cycle activity. Malate synthase catalyzes the conversion of glyoxylate to malate with the consumption of Acetyl-CoA (Fig. 3). Therefore, a decrease in this protein would allow Acetyl-CoA to preferentially enter the TCA cycle instead of producing malate. Malate can also enter the TCA cycle, but generates lower reducing equivalents and ATP. Lower levels of malate synthase could lead to glyoxylate accumulation and subsequent ROS elimination during oxidative stress by a non-enzymatic decarboxylation of glyoxylate [18]. This ROS scavenger role has been described also for other keto-acids, such as pyruvate and alpha-keto-glutarate. This type of defense mechanisms seems to be of special importance for extremophilic microorganisms that do not have detoxifying mechanisms, such as catalases and glutathione [20]. Examples of these are *S. solfataricus* and ammonia oxidizing archaea [21].

Also, there were contradictory changes in proteins with similar functions. For example, Acetyl-CoA *C*-acetyltransferase isoforms AcaB-3 (SSO2062) and AcaB-4 (SSO2377) (Fig. 3) decreased their levels (Table 2). On the other hand, the isoform AcaB-6 (SSO2508) (Fig. 3) increased (Table 1). The activity of these enzymes is related to lipid metabolism, isoleucine degradation and carbon fixation cycle of 3-hydroxypropionate/4-hydroxybutirate. A similar discordance was also reported in the response of *S. solfataricus* to heat shock, were the genes acab-1,-3,-8,-10 decreased their expression, while acab-4,-5,-6 increased [17]. Each isoform is probably involved in different parts of the pathways, but further analysis would be necessary to clarify this point.

PolyP plays many roles in the cell. Perhaps, one of the most important is its ability to replace ATP in some reactions catalyzed by kinases, due to the presence of its high energy bonds analogous to those present in the ATP molecule [1]. It was also reported that the PPK enzyme can catalyze a reverse reaction, where polyP donates a phosphate group to ADP to convert it into ATP in *Escherichia coli* [1]. Although in crenarchaeotes the PPK enzyme has not been described yet, it is likely that an equivalent enzyme should synthesize polyP. Moreover, polyP also has been proposed to have a role in oxidative stress protection. It might act as an inorganic protein chaperone, and form complexes with metals, such as manganese, which can detoxify O_2^- or iron, preventing the formation of ROS through the Fenton's reaction [22]. Due to its aerobic metabolism and the presence of iron in the medium, *S. solfataricus* is constantly exposed to ROS generation. Thus, the lack of polyP should also affect its oxidative stress response.

3.2.2. *Changes in Nucleotide transport and metabolism*

In this category, the exopolyphosphatase (SSO1193) was found up-regulated (Table 1). This was expected since strain M16-PPX constructed here is overproducing its own rPPX to eliminate as much polyP as possible (Fig. 1).

Table 2
Less abundant proteins in *Sulfolobus solfataricus* M16-PPX, lacking polyP, compared to *S. solfataricus* M16.

Accession number	ORF	Function/similarity	Score[a]	Coverage (%)	Peptide number	Fold change (PolyP − /PolyP +)
Metabolism						
Carbohydrate transport and metabolism						
P0CD66	SSO3051	Alpha-glucosidase	158.17	6.64	4	0.65
Q97UF5	SSO3066	Arabinose ABC transporter, arabinose binding protein	174.17	5.16	3	0.58
Q97ZL2	SSO0883	Phosphoenolpyruvate synthase	69.83	8.01	2	0.48
Q97UI8	SSO3029	Uncharacterized protein	142.52	19.78	4	0.4
Q97ZD9	SSO0978	Ribose 5-phosphate isomerase (RpiA)	59.65	11.01	1	0.27
Energy production and conversion						
Q7LXK1	SSO0764	Alcohol dehydrogenase (Zn containing) (Adh-2)	158.52	32.43	13	0.64
P95997	SSO0063	Isopentenyl-diphosphate delta-isomerase	122.58	32.43	13	0.64
Q97XR4	SSO1646	Alcohol dehydrogenase (Zn containing) (Adh-5)	64.83	6.4	1	0.6
Q97YI7	SSO1334	Malate synthase, putative (AceB/mas)	46.27	10.53	4	0.52
Lipid transport and metabolism						
Q97WQ6	SSO2062	Acetyl-CoA *C*-acetyltransferase (Acetoacetyl-CoA thiolase) (AcaB-3)	51.76	7.58	2	0.62
Q97W61	SSO2377	Acetyl-CoA *c*-acetyltransferase (Acetoacetyl-CoA thiolase) (AcaB-4)	69.61	8.31	2	0.6
Coenzyme transport and metabolism						
Q97VJ6	SSO2627	CoA-ligase/coenzyme F390 synthetase, putative	7.9	12.09	1	0.35
Amino acid transport and metabolism						
Q97VA3	SSO2732	Agmatinase (Agmatine ureohydrolase) (SpeB-2)	78.32	9.84	1	0.5
Q980X1	SSO0155	[LysW]-L-2-aminoadipate/[LysW]-L-glutamate Phosphate reductase	48.83	8.81	2	0.46
Q97UG7	SSO3053	Maltose ABC transporter, maltose binding protein	152.7	8.18	5	0.46
Secondary metabolites biosynthesis, transport and catabolism						
Q97UR3	SSO2939	Maleate cis-trans isomerase, probable (MaiA)	48.04	9.09	2	0.58
Cellular processes and signaling						
Cell wall/membrane/envelope biogenesis						
Q97VN5	SSO2583	Sulfolipid biosynthesis protein (SqdB)	49.16	2.06	1	0.49
Defense mechanism						
Q97YC5	SSO1401	Putative CRISPR-associated protein	55.07	5.88	2	0.37
Poorly characterized						
General function predicted only						
Q97UA0	SSO3118	2-dehydro-3-deoxy-D-arabinonate dehydratase	129.02	12.75	4	0.65
Q97Z17	SSO1126	Uncharacterized protein	252.48	37.76	6	0.6
Q980Q0	SSO0235	Uncharacterized protein	56.14	3.44	2	0.52
Q97W84	SSO2373	Uncharacterized protein	60.5	10.58	3	0.36

[a] Score in this table refers to protein score, according to Mascot search engine.

3.2.3. Changes in Coenzyme transport and metabolism

In this group, an increased level of a probable cobalt-precorrin-6B C(15)-methyl transferase (SSO2303), a protein involved in vitamin B12 synthesis was identified (Table 1; not included in Fig. 3). This vitamin is a cofactor for many enzymes with a variety of activities, such as isomerases, methyl transferases and dehalogenases [23]. Additionally, an increase in the enzyme geranylgeranyl pyrophosphate synthase (SSO0061) was observed (Table 1, Fig. 3). A higher level of this enzyme, would increase the concentration of geranyl-PP, geranylgeranyl-PP and farnesyl-PP. These three compounds are relevant for the synthesis of terpenoids and membrane lipids, and also the synthesis of ubiquinone, which are involved in the respiratory chain. They receive electrons from the NADH dehydrogenase and succinate dehydrogenase to transfer them to the cytochrome *bc*1 [24]. D-3-Phosphoglycerate dehydrogenase (SSO0905) also raised its levels (Table 1, Fig. 3). This enzyme participates in the synthesis of serine via a phosphorylative pathway.

Most of these observed changes suggest an increment in the levels of proteins involved in metabolism and energy production due to the lack of polyP in the cell. In this regard, Varela et al. [25] reported increased levels of proteins involved in the TCA cycle and fatty acids degradation in *Pseudomonas* sp. B4 lacking polyP. Moreover, some of the enzymes listed above, such as carbon monoxide dehydrogenase and NADH dehydrogenase (Fig. 3), have an Fe-S central cluster that could be damaged due to ROS generation [20] and therefore increase their levels as seen in Table 1 and Fig. 3.

3.2.4. Changes in Amino acid transport and metabolism

In this category an increase in the levels of serine-pyruvate aminotransferase (AgxT) (SSO2597) was detected (Table 1, Fig. 3). This enzyme was first described to participate in the non-phosphorylative pathway of serine. However, some studies point out that AgxT might participate in the phosphorylative pathway in *S. tokodaii*, a close member of Sulfolobales [26]. The increase in the enzymes related to serine biosynthesis (SSO0905 and SSO2597) not only would affect this particular process, but also other amino acids that can be obtained from it, such as glycine and threonine.

Lastly, another protein with an increased level in *S. solfataricus* cells lacking polyP was the large subunit of Acetolactate synthase (SSO3210) (Table 1. Not shown in Fig. 3). This enzyme is involved in the synthesis of leucine, isoleucine and valine. An increase in enzymes involved in the synthesis of serine and threonine was also reported in *Pyrococcus furiosus* after 5 h of cold shock [27]. These findings could be a late response produced by the accumulation of C-3 and C-4 intermediates, generated by the degradation of glucose in the first hours post-stress. Thus, a possible increase in the synthesis of these amino acids could be related to the activation of glucose and glycogen degradation already discussed in Section 3.2.1.

3.2.5. Changes in Post transcriptional modification, protein turnover and chaperones

In this category, two peroxiredoxins increased their levels: Bcp-4 (SSO2613) and Bcp-2 (SSO2121) (Table 1 and upper left part in Fig. 3).

Both proteins play a central role in protecting *S. solfataricus* from oxidative stress and damage, coupled to the TCA cycle and the respiratory chain [28]. They convert H_2O_2 into H_2O and O_2, regenerate NAD content in the cell and maintain redox balance. The increase in peroxiredoxins has been previously reported in *S. solfataricus* in response to H_2O_2 [29] and in cells of *Pseudomonas* sp. B4 lacking polyP [25]. These findings are in agreement with the role of polyP in protection of cells against oxidative damage [22], and the recently described role of polyP as an inorganic chaperone to avoid protein denaturalization in response to reactive oxygen species [3].

3.2.6. Changes in other categories

Interestingly, in the "cell wall, membrane and envelope biogenesis" category, the sulfolipid biosynthesis protein (SqdB) was down-regulated (Table 2, not included in Fig. 3). This enzyme seems to catalyze the N-glycosylation of some membrane components in Crenarchaeota [30]. Finally, several proteins of unknown function were found up and down-regulated (Tables 1 and 2). Their function and relationship to polyP metabolism remains unidentified. In general, an increment in the glycolytic pathway over the glycogenic pathway was observed in the absence of polyP. Under these conditions, the cell should reduce waste of energy.

More studies are needed to determine the real metabolic state of the cells lacking polyP, since enzyme activities depend not only in their concentration, but also in their induction or inhibition by other factors and in other levels of regulation [31]. Protein phosphorylation/dephosphorylation, is a process that might regulate many enzymes and transcription factor proteins in *S. solfataricus* [31–33], and could also be affected due the lack of polyP [1].

3.3. Possible role of polyP in copper resistance in S. solfataricus

Copper is able to generate ROS by the Fenton reaction [18,34] and it was previously shown that polyP plays a role in copper resistance in archaea [8]. Therefore, it was of interest to assess metal susceptibility of *S. solfataricus* strain M16-PPX. For this, the minimum inhibitory concentration (MIC) of copper was determined in M16-PPX, polyP(−). Cells were grown in Brock medium supplemented with either 0.2% D-arabinose or 0.1% glucose, with different $CuSO_4$ concentrations for 92 h until late exponential phase. MIC was defined as the concentration of copper capable of 50% inhibition of growth. As a control, another recombinant *S. solfataricus* strain overproducing a protein not related to copper resistance was used (data not shown).

As seen in Fig. 4A, M16-PPX grown in glucose has an estimated MIC value of 2 mM Cu. On the contrary, cells grown in D-arabinose, had a MIC value of only 0.75 mM Cu. This result clearly indicates the importance of polyP in copper resistance in *S. solfataricus*.

3.4. Effect of copper in the growth of S. solfataricus M16-PPX PolyP (−)

Cells were allowed to accumulate polyP until they reached an OD_{600} nm of 0.25. They were then transferred to a fresh medium containing either 0.2% D-arabinose or 0.1% glucose as the control condition, and further incubated for 3 h to eliminate all detectable polyP present in the cells. $CuSO_4$ was then added to the medium at the indicated final concentrations and the OD_{600} nm was registered in each case during 48 h. As shown in Fig. 4B, Cu affected preferentially cells lacking polyP.

Since *S. solfataricus* contains fewer canonical type of copper resistance mechanisms (apparently only two cop systems compared with some other microorganisms) [35], it is possible that the proposed polyP-mediated metal detoxification plays an important role in metal resistance, as suggested before [34,36].

3.5. CopA transcriptional levels in S. solfataricus M16 and M16-PPX exposed to copper

CopA is a P-type copper-exporting ATPase that along with CopM (a metal chaperone) and CopT (a transcriptional regulator) forms part of a mechanism for copper resistance in *S. solfataricus* [35]. As already mentioned, polyP seems to play an important role in copper resistance [6,34]. It was of interest therefore, to compare the *copA* transcriptional levels of both M16-PPX and M16 strains grown in the presence of copper.

Both M16 and M16-PPX *S. solfataricus* strains were grown until they reached an OD_{600} nm of 0.3 followed by the induction of *ppx* in the presence of D-arabinose (0.2%) for 3 h. At this time copper was added to have 1 mM final concentration and total RNA was extracted at the times of incubation indicated in Fig. 5. Both kinds of cells (with and without polyP), showed an increased level of transcriptional expression of *copA* in the presence of copper until a maximum value was reached and declining thereafter. However, cells lacking polyP, had a maximum level of *copA* at 20 min, being much higher than that of M16 cells reaching their maximal *copA* levels after 30 min of incubation in the presence of copper. These results suggest that in the absence of polyP, CopA may have an important initial role in the response of *S. solfataricus* to copper.

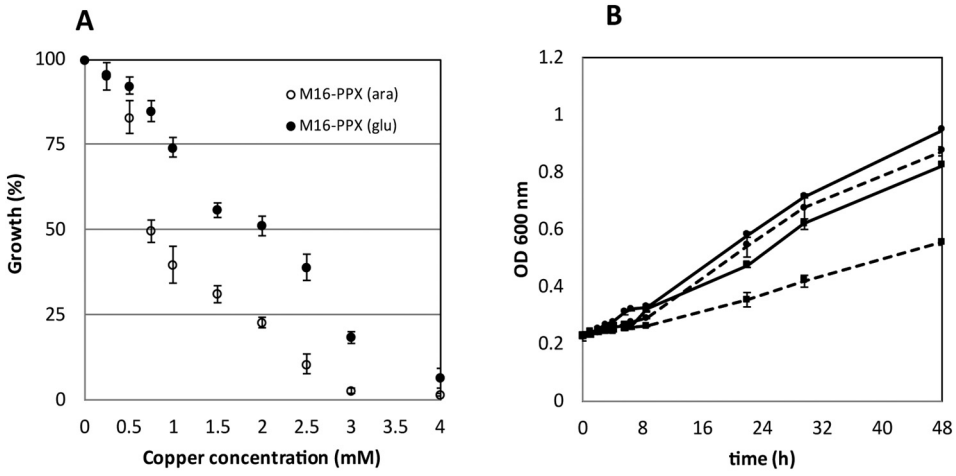

Fig. 4. Effect of $CuSO_4$ on growth of *S. solfataricus* recombinant strain M16-PPX (polyP−). (A) Growth of *S. solfataricus* M16-PPX strain in the presence of 0.2% D-arabinose (○) or 0.1% glucose (●). Copper was added at the indicated final concentrations at the initial time and cell growth was expressed as percentage of an untreated control. (B) An exponentially growing culture of strain M16-PPX was shifted into a medium in the presence of 0.2% D-arabinose (segmented line curves) or 0.1% glucose (solid lines curves). After 3 h of incubation, copper was added (time zero) at the following final concentrations: (●), 0 mM; (■), 1 mM. Three independent determinations were performed for each experiment. The error bars represent the standard deviations.

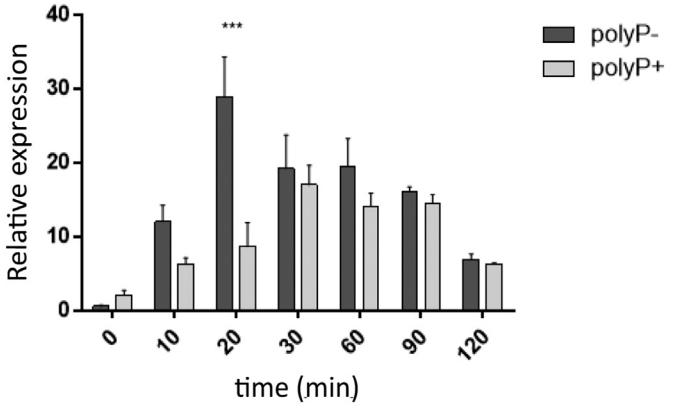

Fig. 5. Changes in the transcriptional expression of *copA* in time after a copper shock in *S. solfataricus* M16 (polyP+) and M16-PPX (polyP−). Copper sulfate (1 mM final concentration) was added to each culture and aliquots of cells were taken at the times indicated to obtain total RNA to determine the transcriptional levels of *copA* by qRT-PCR. Three independent determinations were performed for each experiment. *** p value < 0.001. The bars represent the standard errors.

4. Conclusions

Altogether, the results presented here support that polyP plays a variety of roles in the hyperthermophilic archaeon *S. solfataricus*, and the lack of this polymer triggers a variety of responses, suggesting a similar state to the one caused by oxidative stress.

Regarding copper resistance, as previously reported in the related archaea *S. metallicus*, *M. sedula* and bacteria, polyP may act as a counter ion, helping the expulsion of copper cations through PitA and possibly Pho84-like systems. Recently, a strain of *M. sedula* with a functional PitA and a higher copper resistance than the wild type (who has an incomplete *pitA* gene) has been described [37]. This points out the importance of this phosphate transporter in copper resistance.

Nevertheless further studies will be necessary to unravel the complexity of polyP functions in archaeal cells.

Conflict of interest

The authors declare no conflict of interest.

Transparency document

The Transparency document associated with this article can be found, in online version.

Acknowledgments

Supported by FONDECYT grant no. 1150791.

Appendix A. Supplementary data

Supplementary data to this article can be found online at https://doi.org/10.1016/j.jprot.2018.02.024.

References

[1] A. Kornberg, N.N. Rao, D. Ault-Riché, Inorganic polyphosphate: a molecule of many functions, Annu. Rev. Biochem. 68 (1999) 89–125.
[2] T. Albi, A. Serrano, Inorganic polyphosphate in the microbial world. Emerging roles for a multifaceted biopolymer, World J. Microbiol. Biotechnol. 32 (2016) 1–12.
[3] M. Gray, W.Y. Wholey, N. Wagner, C. Cremers, A. Mueller-Schickert, N. Hock, A. Krieger, E. Smith, R. Bender, J.A. Bardwell, U. Jakob, Polyphosphate is a primordial chaperone, Mol. Cell 53 (2014) 689–699.
[4] S.J.J. Brouns, T.J.G. Ettema, K.M. Stedman, J. Walther, H. Smidt, A.P.L. Snijders, M. Young, R. Bernander, P.C. Wright, B. Siebers, J. van der Oost, The hyperthermophilic archaeon *Sulfolobus*: from exploration to exploitation, in: W. Inskeep, T.R. McDermont (Eds.), Geothermal Biology and Geochemistry in Yellowstone National Park, Proceeding of the Thermal Biology Institute Workshop, Montana State University, 2005, pp. 261–276.
[5] S.V. Albers, M. Jonuscheit, Production of recombinant and tagged proteins in the hyperthermophilic archaeon *Sulfolobus solfataricus*, Appl. Environ. Microbiol. 72 (2006) 102–111.
[6] F. Remonsellez, A. Orell, C.A. Jerez, Copper tolerance of the thermoacidophilic archaeon *Sulfolobus metallicus*: possible role of polyphosphate metabolism, Microbiology 152 (2006) 59–66.
[7] S.T. Cardona, F.P. Chavez, C.A. Jerez, The exopolyphosphatase gene from *Sulfolobus solfataricus*: characterization of the first gene found to be involved in polyphosphate metabolism in Archaea, Appl. Environ. Microbiol. 68 (2002) 4812–4819.
[8] A. Orell, C.A. Navarro, M. Rivero, J.S. Aguilar, C.A. Jerez, Inorganic polyphosphates in extremophiles and their possible functions, Extremophiles 16 (2012) 573–583.
[9] E. Martusewitsch, C.W. Sensen, C. Schleper, High spontaneus mutation rate in the hyperthermophilic archaeon *Sulfolobus solfataricus* is mediated by transposable elements, J. Bacteriol. 182 (2000) 2574–2581.
[10] M. Jonuscheit, E. Martusewitsch, K.M. Stedman, C. Schleper, A reporter gene system for the hyperthermophilic archaeon *Sulfolobus solfataricus* based on a selectable and integrative shuttle vector, Mol. Microbiol. 48 (2003) 1241–1252.
[11] R.J. Almárcegui, C. Navarro, A. Paradela, J.P. Albar, D. Von Bernath, C.A. Jerez, New copper resistance determinants in the extremophile *Acidithiobacillus ferrooxidans*: a quantitative proteomic analysis, J. Proteome Res. (2013) 946–960.
[12] C. Martínez-Bussenius, C.A. Navarro, L. Orellana, A. Paradela, C.A. Jerez, Global response of *Acidithiobacillus ferrooxidans* ATCC 53993 to high concentrations of copper: a quantitative proteomics approach, J. Proteome 145 (2016) 37–45.
[13] A. Orell, F. Remonsellez, R. Arancibia, C.A. Jerez, Molecular characterization of copper and cadmium resistance determinants in the biomining thermoacidophilic archaeon *Sulfolobus metallicus*, Archaea 2013 (2013) 1–16.
[14] H. König, R. Skorko, W. Zillig, W.D. Reiter, Glycogen in thermoacidophilic archaebacteria of the genera *Sulfolobus*, *Thermoproteus*, *Desulfurococcus* and *Thermococcus*, Arch. Microbiol. 132 (1982) 297–303.
[15] I.A. Berg, D. Kockelkorn, W.H. Ramos-Vera, R.F. Say, J. Zarzycki, M. Hügler, B.E. Alber, G. Fuchs, Autotrophic carbon fixation in archaea, Nat. Rev. Microbiol. 8 (2010) 447–460.
[16] Q. She, R.K. Singh, F. Confalonieri, Y. Zivanovic, G. Allard, M.J. Awayez, C.C. Chan-Weiher, I.G. Clausen, B.A. Curtis, A. De Moors, G. Erauso, C. Fletcher, P.M. Gordon, I. Heikamp-de Jong, A.C. Jeffries, C.J. Kozera, N. Medina, X. Peng, H.P. Thi-Ngoc, P. Redder, M.E. Schenk, C. Theriault, N. Tolstrup, R.L. Charlebois, W.F. Doolittle, M. Duguet, T. Gaasterland, R.A. Garrett, M.A. Ragan, C.W. Sensen, J. Van der Oost, The complete genome of the crenarchaeon *Sulfolobus solfataricus* P2, Proc. Natl. Acad. Sci. U. S. A. 98 (2001) 7835–7840.
[17] S. Tacholjian, R.M. Kelly, Dynamic metabolic adjustments and genome plasticity are implicated in the heat shock response of the extremely thermoacidophilic archaeon *Sulfolobus solfataricus*, J. Bacteriol. 188 (2006) 4553–4559.
[18] J. Lemire, A. Alhasawi, V.P. Appanna, S. Tharmalingam, V.D. Appanna, Metabolic defence against oxidative stress: the road less travelled so far, J. Appl. Microbiol. 123 (2017) 798–809.
[19] M. Rolfsmeier, C. Haseltine, E. Bini, A. Clark, P. Blum, Molecular characterization of the alpha-glucosidase gene (*mal*A) from the hyperthermophilic archaeon *Sulfolobus solfataricus*, J. Bacteriol. 180 (1998) 287–1295.
[20] J.P. Cárdenas, F. Moya, P. Covarrubias, A. Shmaryahu, G. Levicán, D.S. Holmes, R. Quatrini, Comparative genomics of the oxidative stress response in bioleaching microorganisms, Hydrometallurgy 127–128 (2012) 162–167.
[21] J.-G. Kim, S.-J. Park, J.S. Sinninghe Damsté, S. Schouten, W.I.C. Rijpstra, M.-Y. Jung, S.-J. Kim, J.-H. Gwak, H. Hong, O.-J. Si, S. Lee, E.L. Madsen, S.-K. Rhee, Hydrogen peroxide detoxification is a key mechanism for growth of ammonia-oxidizing archaea, Proc. Natl. Acad. Sci. U. S. A. 113 (2016) 7888–7893.
[22] M.J. Gray, U. Jakob, Oxidative stress protection by polyphosphate - new roles for an old player, Curr. Opin. Microbiol. 24 (2015) 1–6.
[23] D.A. Rodionov, A.G. Vitreschak, A.A. Mironov, M.S. Gelfand, Comparative genomics of the vitamin B12: metabolism and regulation in prokaryotes, J. Biol. Chem. 278 (2003) 41148–41159.
[24] K.S. Auernik, R.M. Kelly, Identification of components of electron transport chains in the extremely thermoacidophilic crenarchaeon *Metallosphaera sedula* through iron and sulfur compound oxidation transcriptomes, Appl. Environ. Microbiol. 74 (2008) 7723–7732.
[25] C. Varela, C. Mauriaca, A. Paradela, J.P. Albar, C.A. Jerez, F.P. Chávez, New structural and functional defects in polyphosphate deficient bacteria: a cellular and proteomic study, BMC Microbiol. 10 (2010) 1–14.
[26] Y. Shimizu, H. Sakuraba, K. Doi, T. Ohshima, Molecular and functional characterization of D-3-phosphoglycerate dehydrogenase in the serine biosynthetic pathway of the hyperthermophilic archaeon *Sulfolobus tokodaii*, Arch. Biochem. Biophys. 470 (2008) 120–128.
[27] M.V. Weinberg, G.J. Schut, S. Brehm, M.W.W. Adams, S. Datta, Cold shock of a hyperthermophilic archaeon: *Pyrococcus furiosus* exhibits multiple responses to a suboptimal growth temperature with a key role for membrane-bound glycoprotein, J. Bacteriol. 187 (2005) 336–348.
[28] D. Limauro, E. Pedone, I. Galdi, S. Bartolucci, Peroxiredoxins as cellular guardians in *Sulfolobus solfataricus*-characterization of Bcp1, Bcp3 and Bcp4, FEBS J. 275 (2008) 2067–2077.
[29] W.S. Maaty, B. Wiedenheft, P. Tarlykov, N. Schaff, J. Heinemann, J. Robison- Cox, J. Valenzuela, A. Dougherty, P. Blum, C.M. Lawrence, T. Douglas, M.J. Young, B. Bothner, Something old, something new, something borrowed; how the thermoacidophilic archaeon *Sulfolobus solfataricus* responds to oxidative stress, PLoS One 4 (2009) 1–17.

[30] B.H. Meyer, S.V. Albers, Hot and sweet: protein glycosylation in Crenarchaeota, Biochem. Soc. Trans. 41 (2013) 384–392.
[31] C. Brasen, D. Esser, B. Rauch, B. Siebers, Carbohydrate metabolism in *Archaea*: current insights into unusual enzymes and pathways and their regulation, Microbiol. Mol. Biol. Rev. 78 (2014) 89–175.
[32] D. Esser, T.K. Pham, J. Reimann, S.V. Albers, B. Siebers, P.C. Wright, Change of carbon source causes dramatic effects in the phospho-proteome of the Archaeon *Sulfolobus solfataricus*, J. Proteome Res. 11 (2012) 4823–4833.
[33] L. Li, A. Banerjee, L.F. Bischof, H.R. Maklad, L. Hoffmann, A.L. Henche, F. Veliz, W. Bildl, U. Schulte, A. Orell, L.O. Essen, E. Peeters, S.V. Albers, Wing phosphorylation is a major functional determinant of the Lrs14-type biofilm and motility regulator AbfR1 in *Sulfolobus acidocaldarius*, Mol. Microbiol. 105 (2017) 777–793.
[34] A. Orell, C.A. Navarro, R. Arancibia, J.C. Mobarec, C.A. Jerez, Life in blue: copper resistance mechanisms of bacteria and archaea used in industrial biomining of minerals, Biotechnol. Adv. 28 (2010) 839–848.
[35] T.J.G. Ettema, A.B. Brinkman, P.P. Lamers, N.G. Kornet, W.M. de Vos, J. van der Oost, Molecular characterization of a conserved archaeal copper resistance (*cop*) gene cluster and its copper-responsive regulator in *Sulfolobus solfataricus* P2, Microbiology 152 (2006) 1969–1979.
[36] C. Martínez-Bussenius, C.A. Navarro, C.A. Jerez, Microbial copper resistance: importance in biohydrometallurgy, Microb. Biotechnol. 10 (2017) 279–295.
[37] S. McCarthy, C. Ai, G. Wheaton, R. Tevatia, V. Eckrich, R. Kelly, P. Blum, Role of an archaeal PitA transporter in the copper and arsenic resistance of *Metallosphaera sedula*, an extreme thermoacidophile, J. Bacteriol. 196 (2014) 3562–3570.